ELSEVIER

Journal of Photochemistry and Photobiology A: Chemistry 105 (1997) 345–352

Journal of PHOTOCHEMISTRY AND PHOTOBIOLOGY A:CHEMISTRY

Deviations from Lindemann behaviour: photoisomerization dynamics of *trans*-stilbene under collisional gas phase conditions

A. Meyer *, J. Schroeder, J. Troe, M. Votsmeier

Institut für Physikalische Chemie der Universität Göttingen, Tammannstraße 6, D-37077 Göttingen, Germany

Received 2 September 1996; accepted 18 October 1996

Abstract

Systematic fluorescence lifetime measurements of *trans*-stilbene in bath gases nitrogen, methane, ethane and propane at pressures between 1 mbar and 10 bar were analysed by comparison with master equation simulations. The results show that the low-pressure regime of the unimolecular photoisomerization reaction is located well below 1 bar. The increase in the isomerization rate coefficient observed with further increasing pressure contradicts the basic assumption of the Lindemann model and is discussed in terms of the solvent-induced changes of the potential energy surface. The role of restricted intramolecular vibrational energy redistribution (IVR) in determining the observed photoisomerization dynamics is clearly of minor importance. © 1997 Elsevier Science S.A.

Keywords: Energy transfer; Photoisomerization; Solvent effects; Unimolecular reactions

1. Introduction

The photoinduced cis–trans isomerization of ethylenic double bonds is a prototype for a large class of processes of biological and practical importance. In this group of reactions, the isomerization of *trans*-stilbene has been extensively studied under a large variety of physical conditions. These range from the isolated molecule in supersonic jet experiments [1–8], through the gas [9–21] and liquid [15–29] phases, to the high-pressure regime in various solvents [15–19,29–32]. From these experiments, it is known that the isomerization reaction is strongly influenced by specific interactions of the reactant with the surrounding medium. Experiments on the isomerization of stilbene using pressure and temperature variations in polar and non-polar solvents have shown (in contrast with experiments on the next diphenylpolyene homologue diphenylbutadiene [15,20,30,31]) a deviation from the simple Kramers–Smoluchowski theory [33,34], where the rate constant in the high-friction limit is expected to be inversely proportional to the viscosity [15,30]. We have attributed this behaviour to a lowering of the reaction barrier due to the influence of the surrounding medium [35]. Alternative explanations which have been suggested include microscopic friction models [36,37], frequency-dependent friction [29,38], breakdown of the Stokes–Einstein relation [36,37] and multidimensional barrier crossing [39].

A further point of controversy is the interpretation of the fact that the measured rate constants in low-viscosity liquids exceed the value of the high-pressure limit calculated from the specific rate constants $k(E)$ measured in supersonic jet experiments [1,3,40]. Of the possible explanations, the two most probable involve the non-statistical behaviour of the isolated molecule and the influence of the surrounding medium on the effective potential energy surface for the reaction in the high-pressure limit. The first explanation is intimately connected with the rate of intramolecular vibrational energy redistribution (IVR). If IVR is fast on the timescale of the reaction, the measured $k(E)$ values are true microcanonical rate coefficients which can be integrated over the Boltzmann distribution to calculate the correct high-pressure limit of the rate coefficient, k_∞. In addition, we can also estimate a reliable value for the energy barrier of the reaction, E_0, if we plot $k(E)$ vs. the internal vibrational excess energy of the photoexcited stilbene molecule. If, on the other hand, IVR occurs on the timescale of the reaction or is even slower, it may form a bottleneck for the depopulation of observable excited states, and the rate coefficients measured do not correspond to the microcanonical reaction rates [41,42]. In this case, the apparent energy barrier measured in the isolated molecule may be considerably higher than the true barrier height. This helps to explain the faster rates measured in

* Corresponding author. Tel.: (+49) (0)551 393129; fax: (+49) (0)551 393144.

1010-6030/97/$17.00 © 1997 Elsevier Science S.A. All rights reserved
PII S1010-6030(96)04542-X

solution. Since in the energy range corresponding to the expected barrier height IVR is possibly not complete on the reaction timescale [43], a mechanism of this kind may be responsible for the observed discrepancy. Assuming, in contrast, a statistical distribution of energy in the isolated molecule prior to reaction, we used an optimized RRKM [1] fit to the $k(E)$ data to extract the barrier height and calculate k_∞ [40]. In our view, the acceleration of the rate in low-viscosity solvents is caused by solute–solvent interactions which effectively decrease the reaction barrier. From the beam data, we obtain $E_0 = 1300\ cm^{-1}$ [40], whereas measuring the activation energy in supercritical ethane at about 30 bar yields $E_0 = 675\ cm^{-1}$ [24].

The controversial discussion about the isomerization process shows that further investigations of the influence of solvents on the reaction in the regime between the high-pressure limit and isolated molecule conditions are necessary. Balk and Fleming [13] have observed, for the isomerization of stilbene in the presence of methane gas, a thermal rate coefficient exceeding the calculated high-pressure limit for a pressure of 2 bar. Thus we expected to extract more information on the influence of the bath gas on the reaction by measurements of the fluorescence decay in the low-pressure regime using several bath gases. In this way, it should be possible to differentiate between intermolecular interactions and intramolecular processes as slow IVR as a source for the deviations from the statistical models, adding to our understanding of the dynamics of elementary reactions.

The basic mechanism of gas phase reactions can be conveniently described in terms of the Lindemann model, which stresses the importance of collisional energy transfer in unimolecular reactions, such as A → products, and describes the reaction as a three-step process involving collisional activation k_1, collisional deactivation k_{-1} and reaction k_2

$$\begin{array}{ll} A+M & \\ k_1 \downarrow \uparrow k_{-1} & \\ A^*+M & \xrightarrow{k_2} \text{Products} \end{array}$$

As is well known, this model leads to a pressure-dependent rate constant k_{uni} for the unimolecular reaction given by

$$k_{uni} = \frac{k_2 k_1 [M]}{k_2 + k_{-1}[M]} \quad (1)$$

with the two limiting values

$$k_2 \gg k_{-1}[M] \qquad k_{uni} = k_0 = k_1[M] \quad (2)$$

$$k_2 \ll k_{-1}[M] \qquad k_{uni} = k_\infty = \frac{k_2 k_1}{k_{-1}} \quad (3)$$

The low-pressure limit k_0 is controlled by collisional activation; the high-pressure limit k_∞ is determined by the stationary distribution of activated molecules and the rate constant k_2 itself. As a fundamental assumption in this model, the role of the solvent molecules M is limited to collisional energy transfer without direct influence on the reactive step itself. The rate constant k_∞ for a thermal reaction can easily be calculated by integrating the microcanonical specific rate constants $k(E)$ over the normalized Boltzmann distribution $f(E)$ of activated molecules above the reaction barrier

$$k_\infty = \int_{E_0}^{\infty} k(E) f(E) dE \quad (4)$$

to yield a value which is expected to be independent of the bath gas and pressure.

As shown by Ref. [44] and in contrast with former assumptions [17], for a correct analysis of the fluorescence decay curve in the low-pressure regime, collisional energy transfer must be taken into account. This is performed by analysing the decay curves obtained using master equation simulations [45]. Such simulations can describe the interplay between collisional activation, collisional deactivation and the unimolecular reaction which determines the evolution of the S_1 population after excitation [46].

The use of this method for pressure-dependent measurements is appropriate for the examination of solvent specific influences on reactions [20,31]. The applicability of theoretical models can be tested and, in addition, the depopulation of the excited state can be simulated via a master equation. For these reasons, we examined the pressure dependence of the isomerization of *trans*-stilbene in the S_1 state for various bath gases up to pressures of 10 bar by recording the fluorescence decay using the time-correlated single-photon counting technique.

2. Experimental details

The fluorescence decay curves of stilbene after excitation to the S_1 state were obtained with a standard single-photon counting set-up. This is based on an actively mode-locked Nd:YLF laser (Coherent Antares 76) which synchronously pumps a dye laser (Coherent 700). The wavelength of this dye laser used with DCM Special (Lambda Physics) was tuned to 620 nm. The pulses with a duration of 1.5 ps and an average power of 600 mW were frequency doubled in an $LiIO_3$ crystal to give an excitation wavelength of 310 nm. Part (10%) of the excitation pulse was separated and focused on an ultrafast photodiode (Telefunken BPW28) whose output was fed to a constant fraction discriminator (Tennelec TC454) to provide the stop signal at the time to amplitude converter (TAC, Tennelec TC862). The fluorescence of stilbene after excitation was detected with a cooled ultrafast multichannel-plate photomultiplier (MCP, Hamamatsu R3809U). The output pulse of the MCP was amplified and, after discrimination, was used as a start signal for the TAC which was operated in 50 ns sweep mode. The TAC output was digitized in a Wilkinson-type converter (Canberra

[1] RRKM: Rice, Ramsperger, Kassel, Marcus

ADC8713) with 4096 channels and finally registered and analysed in a personal computer. The instrument response function had a full width at half-maximum (FWHM) of 30 ps and, with deconvolution, a time resolution of 20 ps was obtained. For pressure-dependent measurements, a custom made heatable gas cell was used, designed for pressures up to 50 bar and temperatures up to 150 °C [44]. The measurements presented here were performed at a temperature of 323 K in the gas cell, which was controlled via three independent thermocouples. The pressure of the bath gas was monitored with a mechanical manometer. *trans*-Stilbene was obtained from Kodak and further purified via high-performance liquid chromatography (HPLC). The gases were obtained from Messer Grusheim and were used without further purification (purity grades: N_2, 4.6; CH_4, 4.5; C_2H_6, 3.5; C_3H_8, 3.5).

3. Analysis of fluorescence decay curves

3.1. Initial "collision-free" period: k_∞

Under collision-free conditions, the behaviour of the fluorescence decay curve is determined by the initial distribution. The vapour pressure of stilbene at 50 °C is around 1 Torr, i.e. the collision frequency is about 1 μs^{-1}. For the timescale of the reaction (0.5–2 ns), it is therefore reasonable to talk about collision-free conditions. In contrast with measurements in supersonic jet experiments, under thermal conditions the excited distribution in the S_1 state is broad and a non-exponential decay can be expected. Fig. 1 shows the measured decay curve at 323 K after excitation at 310 nm, which is close to the 0–0 transition of the isolated molecule. The calculated decay curve was obtained by summing over the exponential decay of each energy level, determined by $k(E)$, weighted with the relative population and the radiative lifetime

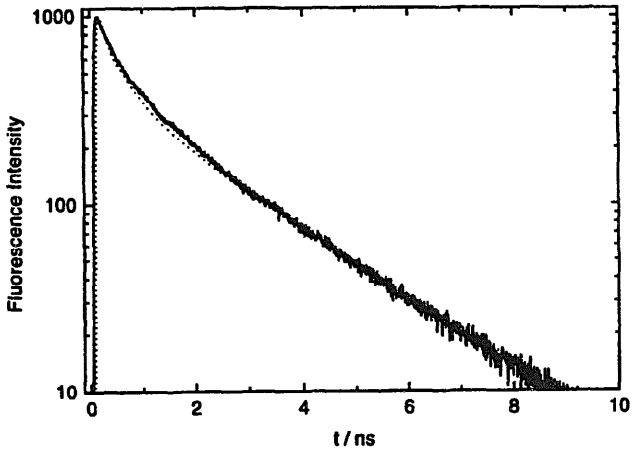

Fig. 1. Logarithmic plot of the multiexponential decay curve of *trans*-stilbene under thermal collision-free conditions (T=323 K, $E_{exc.}$=0). The experimental decay curve (line) is shown together with the model decay curve (dots) calculated by integrating $k(E)$ [30] over the thermal equilibrium Boltzmann distribution (Eq. (4)).

$$g(t) = \frac{\sum_i g(E_i) \exp[-(k_{iso}(E_i) + k_r)t]}{\sum_i g(E_i)} \quad (5)$$

For the radiative lifetime, we used 2.67 ns [2], and for the initial distribution we assumed that the ground state thermal Boltzmann distribution is maintained during excitation to the S_1 state. We neglected varying Franck–Condon factors, an assumption made first by Doany et al. [47] which was later confirmed by Balk and Fleming [13]. The $k(E)$ values were obtained from RRKM calculations, using the optimized frequencies of Troe's fit [40] to the experimental $k(E)$ values [1,3].

The calculated $g(t)$ value was convoluted with the instrument response function $r(t)$ for comparison with the measured fluorescence decay curve

$$I(t) = \int_0^t g(t) r(t-\tau) d\tau \quad (6)$$

In this way, we obtained a reasonable fit without larger deviations considering that we used no fitting parameters except the amplitude of the decay curve. This good agreement using a Boltzmann equilibrium distribution in the S_1 state was also reported by Balk and Fleming [13], and confirms the assumption that the initial distribution is maintained during excitation and that the Franck–Condon factors can be neglected. Therefore our initial distribution in the excited state is the thermal equilibrium distribution after excitation to the 0–0 transition. This allows us to extract the thermal rate constant k_∞ from the initial slope of the decay curve, which is determined by the sum of the radiative rate k_r and the high-pressure limit k_∞

$$k_{exp} = k_\infty + k_r \quad (7)$$

Within the Lindemann model, the value of k_∞ must be independent of the bath gas and pressure. The following pressure- and bath gas-dependent measurements provide the possibility to test the hypothesis that there is no influence on the initial decay rate and the applicability of statistical theories.

For modelling the induction period, we must analyse the fluorescence decay by master equation simulations [44]. The change in the concentration of reactant molecules in energy state E is equal to the sum of depletion, replenishment and reaction [46]. The progress of the reaction is simply monitored by observing $g(t)$

$$\frac{dg(E_i,t)}{dt} = Z\sum_k P(E_i \leftarrow E_k) g(E_k,t) - Z g(E_i,t) - k(E_i) g(E_i,t) \quad (8)$$

The master equation represents the population and depopulation of each energy level, determined by collisional activation, collisional deactivation and the reaction to the products. $k(E)$ represents the reaction rate corresponding to each energy level. The values were calculated using the optimized RRKM fit of Troe [40] as described above (model

C). The collision frequency Z was calculated using simple gas phase collision theory and Lennard–Jones (LJ) parameters [48]. The LJ diameter of stilbene was calculated from the critical data obtained by an increment method [49]. For the initial distribution $g(t=0)$, we used the thermal equilibrium distribution of the ground state excited to the S_1 state. The energy transfer probability function $P(E,E')$ was assumed to be an exponential of the form [45]

$$P(E_i \leftarrow E_k) = N \exp\left(-\frac{\Delta E}{\alpha}\right) \qquad E_k > E_i \tag{9}$$

In this expression, the parameter α determines the average energy transferred per downward collision and is assumed to be independent of energy. The value of α was determined from the Lindemann low-pressure limiting rate constants k_0 obtained from the long time behaviour. In this region, the behaviour is mostly determined by the distribution maintained and therefore the average energy transferred per collision [44]. Detailed balance was used for the relation between upward and downward collisions

$$P(E_k \leftarrow E_i) = N \frac{g(E_i)}{g(E_k)} \exp\left(-\frac{\Delta E}{\alpha}\right) \qquad E_k > E_i \tag{10}$$

3.2. Steady state regime: k_{uni}

Adding a buffer gas will change the decay curves. As before, the excitation of the thermal ground state distribution to the first excited state leads to an initial Boltzmann distribution, as shown in Fig. 2. Following the Lindemann model, at low pressures, the collision rate is not high enough to maintain this broad distribution. Because of the low isomerization barrier of stilbene, $E_0 = 1300\ cm^{-1}$ [40], a large fraction of the molecules possesses an internal energy higher than the barrier. The molecules disappear with a high rate constant $k(E)$, which causes a fast initial decay of the fluorescence. During this time, the relative population of the high vibrational levels decreases and a narrower stationary distribution with a lower average energy is established. Eventually, the fluorescence decay slows down and, after the initial induction period, a single exponential decay should be observed, which is determined by the stationary distribution maintained by the collisions (Fig. 2) and can be characterized by the thermal unimolecular rate constant k_{uni}.

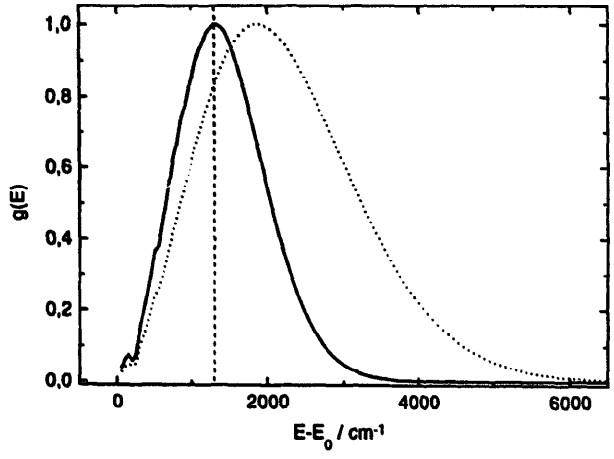

Fig. 2. Vibrational distribution in the S_1 state of *trans*-stilbene after excitation ($T = 323$ K, $E_{exc.} = 0$) (dots) and after establishment of a stationary distribution (approximately 2 ns) at a pressure of 0.6 bar nitrogen (line). The vertical broken line corresponds to the barrier for the isomerization of the isolated molecule ($E_{barrier} = 1300\ cm^{-1}$).

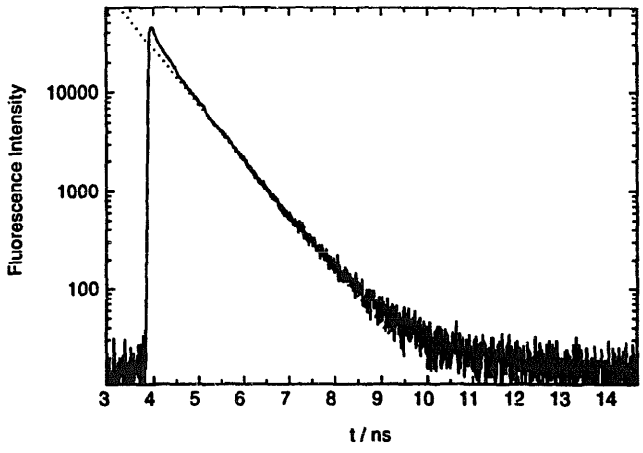

Fig. 3. Logarithmic plot of the fluorescence decay curve (line) of *trans*-stilbene with 0.6 bar nitrogen ($T = 323$ K, $E_{exc.} = 0$). The first part is determined by a multiexponential decay and the long time behaviour by a monoexponential decay. Also shown is a monoexponential fit to the long time behaviour (dots), leading to a rate constant of $0.89\ ns^{-1}$ for the isomerization after subtracting the radiative lifetime $k_r = 0.37\ ns^{-1}$.

A fluorescence decay curve of stilbene in nitrogen at 0.6 bar and 323 K is shown in Fig. 3. It illustrates the induction period with a fast non-exponential decay at short times and the following monoexponential decay at long times. From a simple monoexponential fit to the long time behaviour, we can extract the lifetime of the S_1 state. Subtracting the radiative rate gives the unimolecular rate constant for the isomerization reaction (Eq. (7)). The intersystem crossing rate in *trans*-stilbene is small and can be neglected for our purposes.

4. Results and discussion

The unimolecular rate constants k_{uni} for several pressures of nitrogen up to 1 bar, obtained from the long time behaviour, are plotted in Fig. 4. The pressure dependence is clearly linear and means that we are in the low-pressure regime of the Lindemann model. For higher pressures, the onset of the Lindemann fall-off is observed. From the slope of the linear pressure dependence, the activation rate constant k_1 can be extracted: $1.4\ bar^{-1}\ ns^{-1}$. Turning to the initial slope, which contains k_∞, we observe a strong pressure dependence shown in Fig. 5, which contradicts the statistical model described above. A comparison with master equation simulations, using the same $k(E)$ values as above for collision-free conditions and an initial Boltzmann distribution, clearly demonstrates

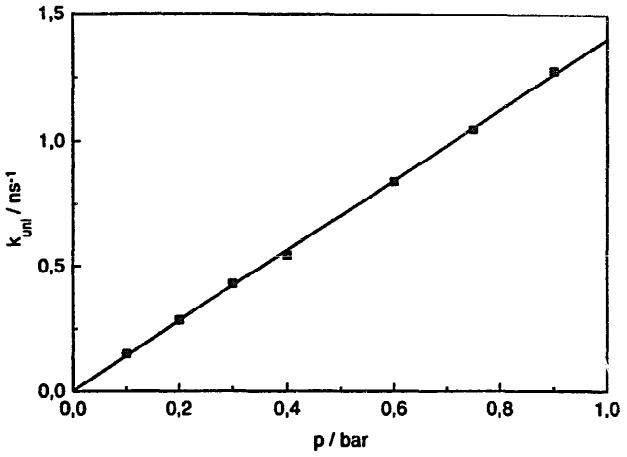

Fig. 4. Unimolecular rate constants k_{uni} for the isomerization of *trans*-stilbene as a function of nitrogen pressure (■) obtained from the long time behaviour. The linear fit (line) yields an activation rate of 1.4 bar^{-1} ns^{-1}. Because of the linear pressure dependence and excitation at the 0–0 origin, this regime corresponds to the low-pressure limit of the Lindemann model.

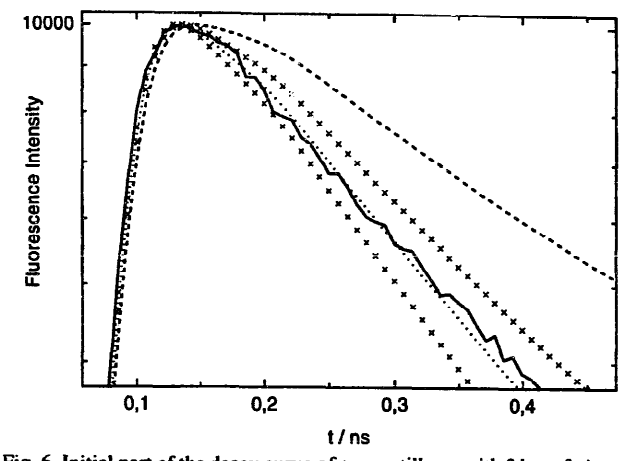

Fig. 6. Initial part of the decay curve of *trans*-stilbene with 3 bar of nitrogen (line, $T = 323$ K, $E_{exc.} = 0$) and calculated decay curves obtained from master equation simulations and convolution with the instrument response function (Eq. (6)). The slowest decay (broken line) was obtained using $k(E)$ from an optimized RRKM fit to the experimental data [30]. The best fit was obtained with a $k(E)$ set corresponding to a barrier of approximately 1180 cm^{-1} (dots). The other decay curves were calculated with ± 10% deviations for $k(E)$ from the optimal fit (crosses).

that the observed decay at a pressure of 3 bar nitrogen is much faster than the calculated value (Fig. 6). Thus the role of collisions does not seem to be limited merely to energy redistribution.

In the next step, a set of pressure-dependent $k(E,E_0(p))$ values was used to fit the calculated decay iteratively to the initial part of the measured decay curves. As a result, we obtained a pressure dependence of the high-pressure limit $k_{th}(p)$ with an accuracy better than 10% (Fig. 6). Using this procedure, a linear dependence for $k_{th}(p)$ on the nitrogen pressure was obtained (Fig. 7). The slope was determined to be 0.91 bar^{-1} ns^{-1} and is less than the slope for k_0.

A similar pressure dependence of $k_{th}(p)$ was also observed for other bath gases. The results of the fitting procedure for the alkanes methane, ethane, and propane as bath gases are plotted in Fig. 8. Evidently, the slope is dependent on the bath gas properties. For ethane and propane, a turnover to a new upper limit of the reaction rate occurs at pressures of 8 bar and 5 bar respectively. Measurements up to higher pressures with nitrogen and methane will also show whether an upper limit can be reached for these gases. In comparison with former measurements in the liquid phase [15], the upper limits here are lower than those reached from the high-viscosity side, as discussed elsewhere [44]. Both series of measurements, however, show a dependence of the upper limit on the bath gas.

In summary, we do not observe a simple fall-off behaviour marked by a transition from a low-pressure regime with $k_0 \propto p$ due to collisional activation to a constant high-pressure limit k_∞. Instead, we find a transition from the low-pressure limit $k_0 = k_1 p$ to $k_{th} \propto$ constant $\times p$, which finally turns into a limiting value k_{sol} = constant at solvent densities at which we

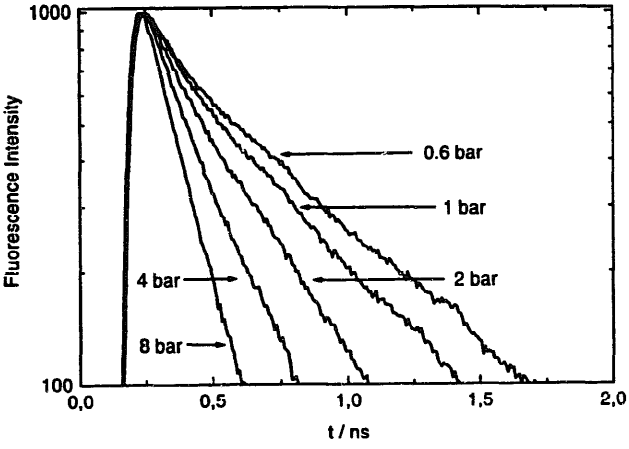

Fig. 5. Initial decay of *trans*-stilbene fluorescence for several pressures of nitrogen (0.6–8 bar, $T = 323$ K, $E_{exc.} = 0$). The pressure dependence of the initial decay rate is in contrast with the Lindemann model.

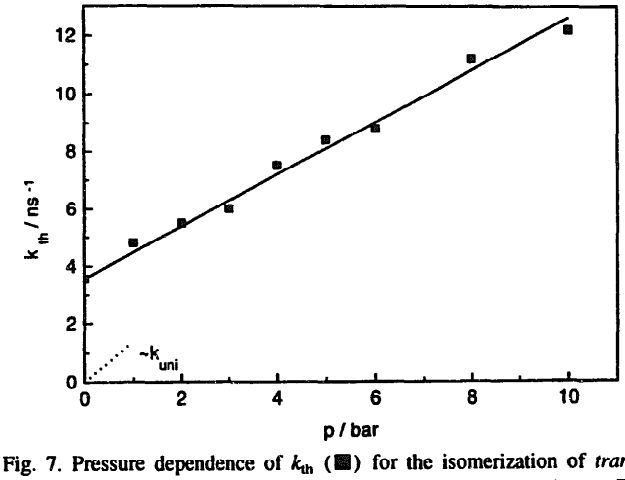

Fig. 7. Pressure dependence of k_{th} (■) for the isomerization of *trans*-stilbene, obtained from the initial decay with nitrogen as bath gas. For comparison, we also show the low-pressure regime (dots) of Fig. 4. A linear regression (line) to $k_{th}(p)$ gives a slope of 0.91 bar^{-1} ns^{-1} which is lower than the slope of $k_{uni}(p)$ in the low-pressure regime of 1.4 bar^{-1} ns^{-1}.

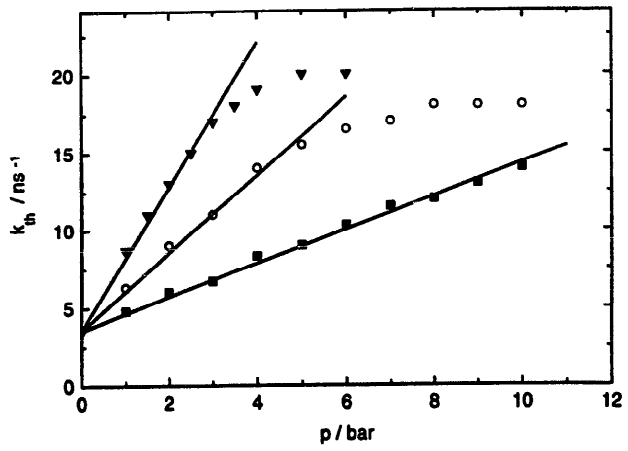

Fig. 8. Pressure dependence of k_{th} for the isomerization of *trans*-stilbene in several alkanes, obtained from the initial fluorescence decay in methane (■), ethane (○) and propane (▼).

might expect a high abundance of stilbene–solvent clusters having an almost intact first solvation shell [15]. The key question to answer concerns the origin of the peculiar pressure dependence. As mentioned above, there are basically two possibilities: solvent-induced enhancement of IVR or changes in the effective potential energy surface for the reaction.

First, we consider the hypothesis that IVR is incomplete on the timescale of the barrier crossing process at low densities (a few millibars of bath gas pressure) at excitation energies only slightly above $v' = 0$ in the S_1 state of stilbene. In this case, increasing the pressure and hence the collision frequency will probably assist IVR which will eventually become fast enough to be essentially complete on the reaction timescale. The increase in rate, $k_{th} \propto$ constant $\times p$, will reflect the enhancement of the rate of IVR, and the limiting value reached will eventually correspond to the true high-pressure limit, such that $k_{sol} = k_\infty$. If this is the only effect of the solute–solvent interaction, k_{sol} should have the same value in all solvents, which is not observed (Fig. 7 and Fig. 8). Therefore we conclude that solvent-induced enhancement of the IVR rate cannot be the only effect causing the observed $k_{th}(p)$ dependence. However, we are not in a position to rule it out entirely.

Next, we consider solvent-induced changes in the effective potential energy surface for the reaction. Here we must consider two possible solvent effects: (1) "static" lowering of the potential energy barrier in the S_1 state [35] with increasing solvent density; (2) a dynamic effect changing the effective reaction path by affecting the curve crossing on a diabatic energy surface [8].

On the basis of our results, we believe that we can rule out the second alternative as extremely unlikely, because the enhancement of $k_{th}(p)$ takes places at pressures of a few bars where the collision frequency is still fairly low. Since the increase in the rate coefficient in this case would be caused by an enhancement of curve hopping in the crossing point region as the motion through this part of the potential energy surface is more and more retarded, at the gas phase-like viscosities under our experimental conditions, this mechanism would be expected to have only a negligible effect.

Therefore we favour the barrier shift effect as the main cause of the increase in k_{th} with p. We have already shown that it definitely plays a major role in the liquid phase photoisomerization dynamics of *trans*-stilbene in non-polar [15] and polar [30] solvents. From these results, we can conclude that the barrier is highly susceptible to the polarizability of the solvent environment, which means that the S_1 potential energy surface of *trans*-stilbene most probably has a highly dipolar character in the barrier region, indicating a fairly "late" barrier along the reaction path. Recently, we estimated the dipole moment of photoexcited *trans*-stilbene to be 22 D in the barrier region, which implies an enormous amount of charge rearrangement along the reaction path from the virtually non-polar trans conformation to the barrier [30].

As a first approximation, we can assume that a similar charge separation also takes place in the isolated molecule, i.e. that there is no or little "feedback" due to solvent rearrangement to amplify this process. In this case, we may estimate the electrostatic energy required to bring about the necessary lowering of the barrier, e.g. at a pressure of 10 bar in ethane. From measurements of the red shift of the absorption spectrum of *trans*-stilbene in ethane [50], we can calculate that the S_1 state of stilbene in the trans conformation is lowered by 100 cm^{-1} with respect to its position in pure stilbene vapour. From our value of k_{th} ($p = 10$ bar, ethane), we know that the barrier height must be 950 cm^{-1}. For simplicity, we assume that the dipole moment of stilbene in trans S_1 is zero and that the electronic polarizability of S_1 stilbene does not change along the reaction path (definitely a gross oversimplification). This means that we also obtain 100 cm^{-1} lowering of the potential energy surface all along the reaction path, and we need an additional 350 cm^{-1} decrease of the barrier due to the hypothetical dipole moment of stilbene at the barrier. Using standard solvent shift models [51], we can calculate $\mu_{barrier}$ according to

$$\frac{\mu^2 f(\varepsilon)}{4\pi\varepsilon_0 A^3} = \Delta E \tag{11}$$

For the stilbene radius $\sigma = A/2$, we used the LJ radius of 7.8 Å calculated from the critical parameters estimated with the increment method [49]. The $f(\varepsilon)$ function was given in Ref. [49] for ethane at a pressure of 10 bar

$$f(\varepsilon) = \frac{\varepsilon - 1}{\varepsilon + 2} = \frac{n^2 - 1}{n^2 + 2} \tag{12}$$

Using the simplifying assumptions listed above, we calculated $\mu_{barrier} = 28$ D for *trans*-stilbene in the barrier region of the S_1 state. This value represents an upper limit and therefore compares well with the value of 22 D obtained from measurements of the barrier shift in compressed alcohols [30]. We used the homogeneous solvent density in estimating this value. It is very likely, however, that the local density

of ethane in the vicinity of stilbene is higher than the average density. This would lead to an increase in the effective $f(\varepsilon)$ used in Eq. (12) and hence to a lower value of $\mu_{barrier}$, giving better agreement with the value estimated from liquid phase measurements.

In addition to the deviation from simple Lindemann behaviour, the low-pressure regime for the isomerization of *trans*-stilbene was observed for the first time. This low-pressure regime is located in the region below 1 bar and not at pressures up to approximately 10 bar as assumed previously [19]. At such high pressures, a further increase in the rate constant must be attributed to the type of solvent influence on the reaction as described above and is not caused by further collisional activation. For pressures above 2 bar, calculations have shown that the stationary distribution is equal to the thermal initial distribution and can be maintained by collisions. Increasing the pressure and collision frequency in this regime has no effect within the Lindemann model. Additional evidence for this conclusion is the fact that the measured decay curves are monoexponential in this pressure regime.

5. Conclusions

The low-pressure limit and conventional fall-off region are clearly situated well below a pressure of 1 bar, and the observed pressure dependence of the thermal rate coefficient for the reaction in the S_1 state above 1 bar must be attributed to solvent-induced variations of the effective barrier height for S_1 isomerization. This conclusion confirms solvent shift models proposed on the basis of liquid phase measurements. The experiments show beyond any doubt that solvent-assisted IVR alone cannot be responsible for the order of magnitude enhancement of the reaction rate and probably only plays a minor role. This result also has consequences for the interpretation of recent measurements on the dynamics of selected jet-cooled stilbene–hexane clusters [52]. In addition, for the first time, the true low-pressure regime, located in the millibar region, was observed for this reaction.

Acknowledgements

Financial support by the Deutsche Forschungsgemeinschaft (SFB 357 "Molekulare Mechanismen Unimolekularer Prozesse") is gratefully acknowledged.

References

[1] J.A. Syage, W.R. Lambert, P.M. Felker, A.H. Zewail and R.M. Hochstrasser, Chem. Phys. Lett., 88 (1982) 268.
[2] J.A. Syage, P.M. Felker and A.H. Zewail, J. Chem. Phys., 81 (1984) 4685, 4706.
[3] A. Amirav and J. Jortner, Chem. Phys. Lett., 95 (1983) 295.
[4] T.J. Majors, U. Even and J. Jortner, J. Chem. Phys., 81 (1984) 2330.
[5] S.H. Courtney, M.W. Balk, L.A. Philips, S.P. Webb, D. Yang, D.H. Levy and G.R. Fleming, J. Chem. Phys., 88 (1988) 6697.
[6] L.R. Khundkar, R.A. Marcus and A.H. Zewail, J. Phys. Chem., 87 (1983) 2473.
[7] N.F. Scherer, J.W. Perry, F.E. Doany and A.H. Zewail, J. Phys. Chem., 89 (1985) 894.
[8] P.M. Felker and A.H. Zewail, J. Phys. Chem., 89 (1985) 5402.
[9] T.S. Zwier, E.M. Carrasquillo and D.H. Levy, J. Chem. Phys., 78 (1983) 5493.
[10] N.F. Scherer, J.P. Shepanski and A.H. Zewail, J. Chem. Phys., 81 (1984) 2181.
[11] J.W. Perry, N.F. Scherer and A.H. Zewail, Chem. Phys. Lett., 103 (1983) 1.
[12] B.I. Greene, R.M. Hochstrasser and R.B. Weisman, J. Chem. Phys., 71 (1979) 544.
[13] M.W. Balk and G.R. Fleming, J. Phys. Chem., 90 (1986) 3975.
[14] S.H. Courtney and G.R. Fleming, J. Chem. Phys., 83 (1985) 215.
[15] J. Schroeder, D. Schwarzer, J. Troe and F. Voß, J. Chem. Phys., 93 (1990) 2393.
[16] J. Schroeder and J. Troe, Chem. Phys. Lett., 116 (1985) 453.
[17] G. Maneke, J. Schroeder, J. Troe and F. Voß, Ber. Bunsenges. Phys. Chem., 89 (1985) 896.
[18] G.R. Fleming, S.H. Courtney and M.W. Balk, J. Stat. Phys., 42 (1986) 83.
[19] M. Lee, G.R. Holtom and R.M. Hochstrasser, Chem. Phys. Lett., 118 (1985) 359.
[20] J. Schroeder, Ber. Bunsenges. Phys. Chem., 95 (1991) 233.
[21] B.I. Greene, R.M. Hochstrasser and R.B. Weisman, Chem. Phys., 48 (1980) 289.
[22] V. Sundström and T. Gillbro, Chem. Phys. Lett., 109 (1984) 538.
[23] V. Sundström and T. Gillbro, Ber. Bunsenges. Phys. Chem., 89 (1985) 222.
[24] J.M. Hicks, M.T. Vandersall, E.V. Sitzmann and K.B. Eisenthal, Chem. Phys. Lett., 135 (1987) 413.
[25] M. Sumitani, N. Nakashima, K. Yosihara and S. Nagakura, Chem. Phys. Lett., 51 (1977) 183.
[26] M. Sumitani, N. Nakashima and K. Yoshihara, Chem. Phys. Lett., 68 (1979) 255.
[27] R.M. Hochstrasser, Pure Appl. Chem., 52 (1980) 2892.
[28] S.H. Courtney and G.R. Fleming, Chem. Phys. Lett., 103 (1984) 443.
[29] S.P. Velsko and G.R. Fleming, J. Chem. Phys., 76 (1982) 3553.
[30] R. Mohrschladt, J. Schroeder, D. Schwarzer, J. Troe and P. Vöhringer, J. Chem. Phys., 101 (1994) 7566.
[31] Ch. Gehrke, J. Schroeder, D. Schwarzer, J. Troe and F. Voß, J. Chem. Phys., 92 (1990) 4805.
[32] L.A. Brey, G.B. Schuster and H.G. Drickamer, J. Am. Chem. Soc., 101 (1979) 129.
[33] H.A. Kramers, Physica, 7 (1940) 284.
[34] S. Chandrasekhar, Rev. Mod. Phys., 15 (1943) 1.
[35] J. Schroeder and J. Troe, Chem. Phys. Lett., 116 (1985) 453.
[36] S.H. Courtney, S.K. Kim, S. Canonica and G.R. Fleming, J. Chem. Soc., Faraday Trans. 2, 82 (1986) 2065.
[37] M. Lee, A.J. Bain, P.J. McCarthy, C.H. Han, J.N. Haseltine, A.B. Smith III and R.M. Hochstrasser, J. Chem. Phys., 85 (1986) 4341. M. Lee, N. Haseltine, A.B. Smith III and R.M. Hochstrasser, J. Am. Chem. Soc., 111 (1989) 5044.
[38] G. Rothenberger, D.K. Negus and R.M. Hochstrasser, J. Chem. Phys., 79 (1983) 5360.
[39] N. Agmon and R. Kosloff, J. Phys. Chem., 91 (1987) 1988.
[40] J. Troe, Chem. Phys. Lett., 114 (1985) 241.
[41] S. Nordholm, Chem. Phys., 137 (1989) 109.
[42] K. Bolton and S. Nordholm, Chem. Phys., 203 (1996) 101.
[43] P.M. Felker, W.R. Lambert and A.H. Zewail, J. Chem. Phys., 82 (1985) 3003.
[44] A. Meyer, J. Schroeder, J. Troe and M. Votsmeier, to be published.

[45] R.G. Gilbert and S.C. Smith, Theory of Unimolecular and Recombination Reactions, Blackwell Scientific Publications, Oxford, 1990.
[46] I. Oref and D.C. Tardy, Chem. Rev., 90 (1990) 1407.
[47] F.E. Doany, B.I. Greene, Y. Liang, D.K. Negus and R.M. Hochstrasser, Picosecond Phenomena II, Springer, New York, 1980.
[48] D. Ben-Amotz and D.R. Herschbach, Phys. Chem., 94 (1990) 1038.
[49] R.C. Reid, J.M. Prausnitz and B.E. Poling, The Properties of Gases and Liquids, McGraw-Hill, New York, 1987.
[50] D. Schwarzer, Diplom Thesis, Göttingen, 1986.
[51] C. Reichhardt, Solvents and Solvent Effects in Organic Chemistry, VCH, Weinheim, 1988.
[52] Ch. Lienau, A.A. Heikal and A.H. Zewail, Chem. Phys., 175 (1993) 171.